Supplementary information

Tuning the Morphology of Segmented Block copolymers with Zr-MOF nanoparticles for Durable and Efficient Hydrocarbon Separation Membranes

Ali Pournaghshband Isfahani,[ab] Morteza Sadeghi,[c] Somaye Nilouyal,[ab] Guoji Huang,[ab] Ansori Muchtar,[ab] Masateru M. Ito,[ab] Daisuke Yamaguchi,[ab] Easan Sivaniah,*[ab] and Behnam Ghalei*[ab]

a. Institute for Integrated Cell-Material Sciences (iCeMS), Kyoto University, Kyoto,606-8501, Japan
b. Department of Molecular Engineering, Graduate School of Engineering, Kyoto University, Kyoto, Japan
c. Department of Chemical Engineering, Isfahan University of Technology, Isfahan, 84156-83111, Isfahan, Iran
* Corresponding authors. Email: esivanah@icems.kyoto-u.ac.jp; bghalei@icems.kyoto-u.ac.jp; Tel: +81-75-753-9865

Supplementary information

1.1. Gas permeation test

The gas permeability of all membranes was measured using a constant volume-variable pressure method. The permeation gas cell comprises a stainless steel holder with an effective area of 2cm^3 (Millipore XX4502500) equipped with gas and vacuum lines [1]. The changes in pressure and temperature are recorded by an absolute pressure sensor (Keller PAA33X). Gas transport in the polyurethane membranes is explained by the solution-diffusion mechanism, where the gas permeability is the product of gas diffusivity (D) and gas solubility (S) coefficients: $P_i=D_i \times S_i$. The gas permeation coefficient is calculated from equation S1:

$$P = J_i \frac{l}{\Delta p} = 10^{10} \frac{273.15}{76} \frac{V}{AT} (\frac{dp}{dt}) \frac{l}{\Delta p} \quad \text{(S1)}$$

In eq.S1, J_i is the gas flux, l is the membrane thickness, and Δp is the pressure drop between the feed and permeate side of the membrane. Besides, $\left(\frac{dp}{dt}\right)$ is the pressure difference rate in the steady-state gas transmission through the membrane. V, A, and T represent the permeate volume, the effective area of the membrane, and measurement temperature, respectively. The gas permeability unit is mol.m.m^{-2}.s^{-1}.Pa^{-1} or barrer=10^{-10}cm^3(STP)cm cm^{-2}s^{-1}cmHg^{-1}.

The ideal selectivity of the membrane $\alpha_{i/j}$ is calculated by the ratio of permeability coefficients of two individual gases i and j, which also can be written as the product of the diffusivity and solubility coefficients:

$$\alpha_{i/j} = \frac{P_i}{P_j} = \frac{D_i S_i}{D_j S_j} \quad \text{(S2)}$$

The diffusivity coefficient of each gas can be calculated from the time-lag method:

$$D_i = \frac{l^2}{6\theta} \quad \text{(S3)}$$

Linear extrapolation of the slope from the steady-state region of p vs. t curve and compute the x-axis intercept gives θ.

The mixed gas separation properties of the membrane were determined for CO_2/N_2 (50/50 vol.%) and CO_2/H_2 (50/50 vol.%) at 4 bar and 25°C. The stage cut was kept less than 1% to ensure that the feed gas composition does not change over time. The permeate was analyzed by GC gas chromatography and the separation factor can be obtained by equation S4:

$$\alpha_{i/j} = \frac{y_i / y_j}{x_i / x_j} \quad \text{(S4)}$$

where x and y are the gas mol fractions in the feed and permeate, respectively.

Supplementary information

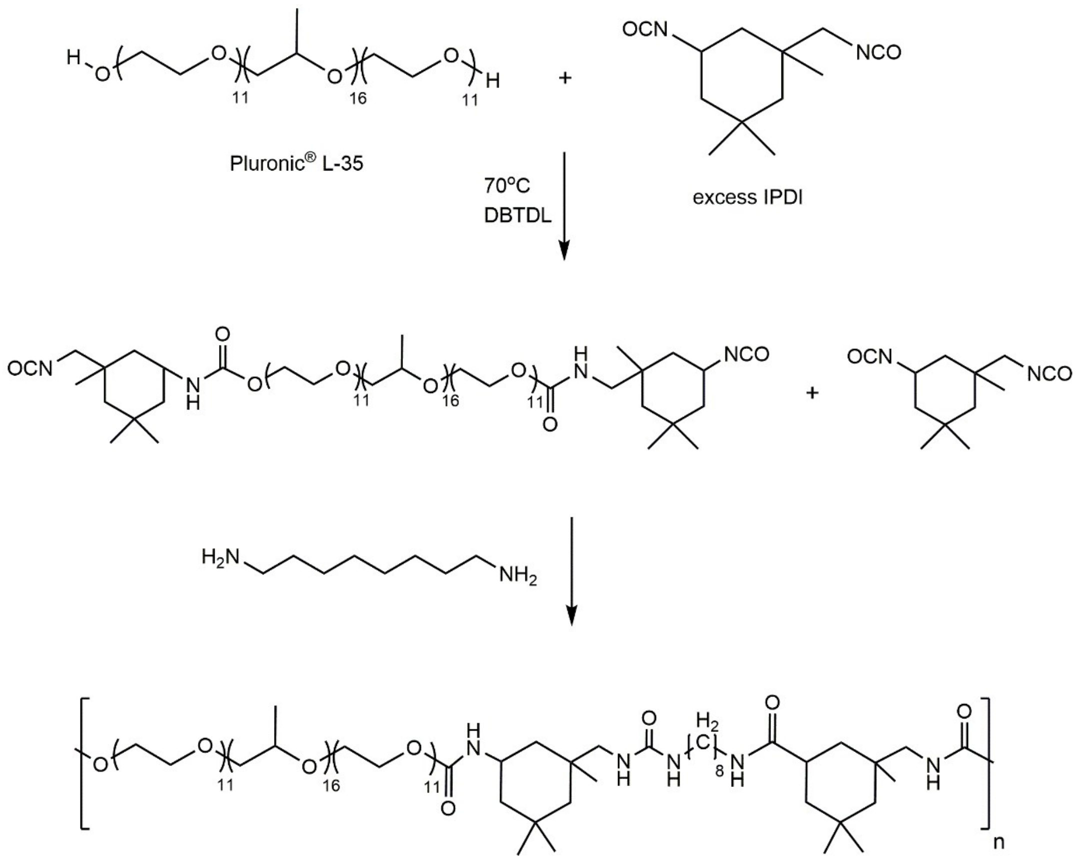

Fig. S1 Schematic representation of PU synthesis

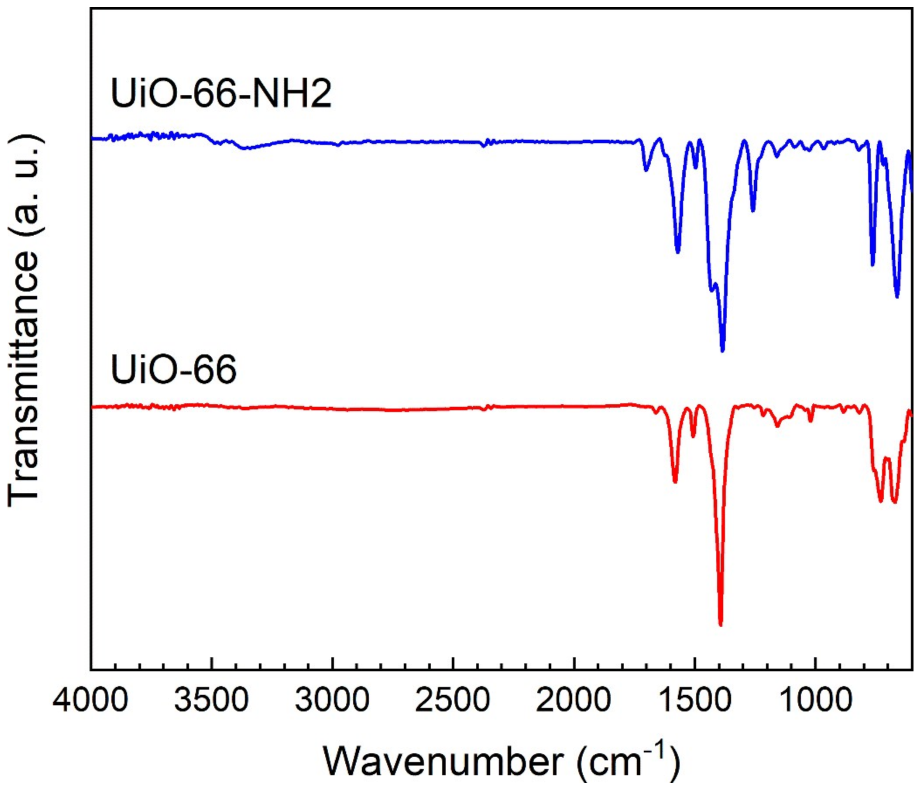

Fig. S2 FTIR spectra of non-functionalized UiO66 and amine-functionalized UiO66 particles.

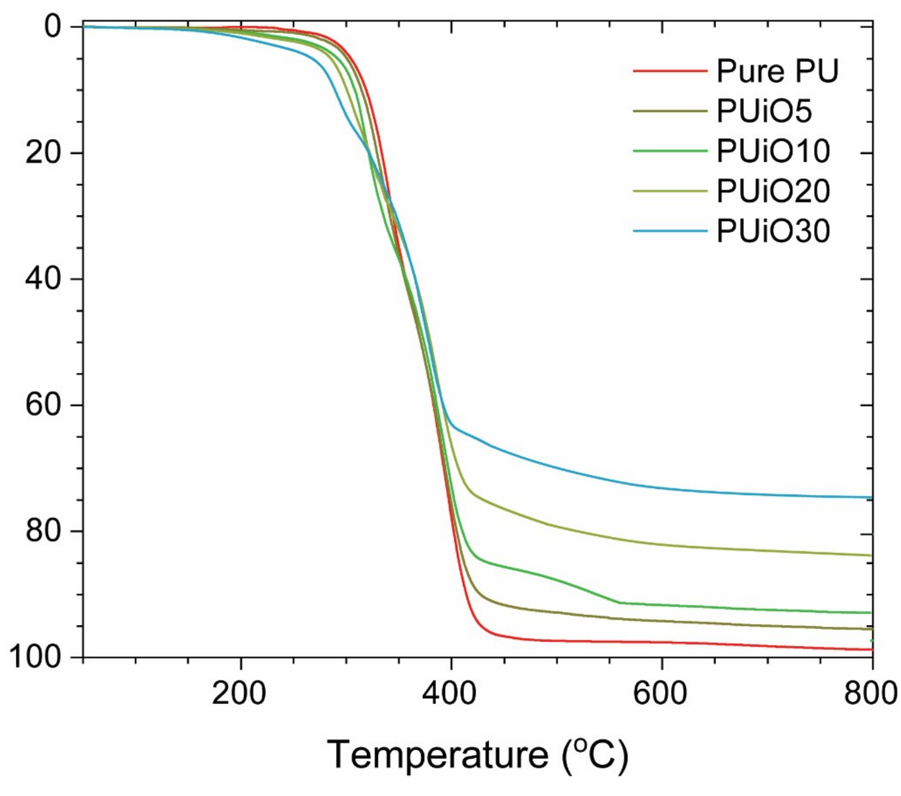

Fig. S3 TGA thermograms of the PU/UiO66 MMMs

Supplementary information

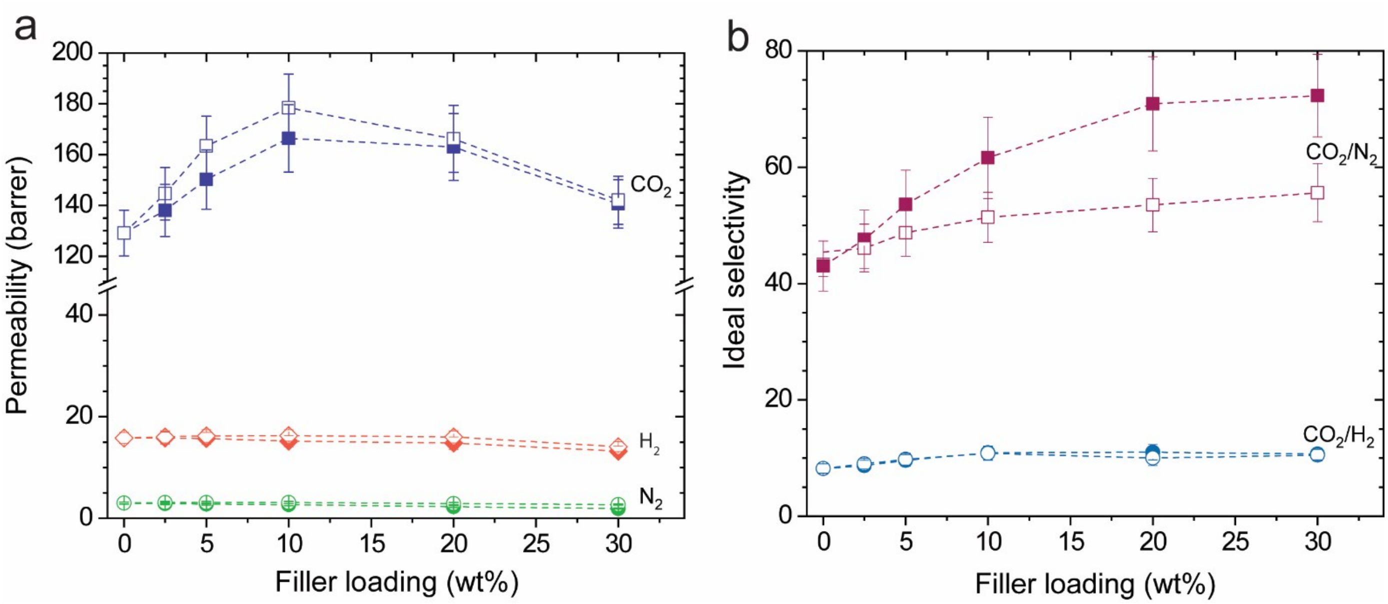

Fig. S4 (a) Gas permeability of CO_2, N_2 and H_2 ,and (b) CO_2/N_2 and CO_2/H_2 ideal selectivity in MMMs as a function of non-functionalized UiO66 (open symbols) and UiO66-NH2 loadings (filled symbols).

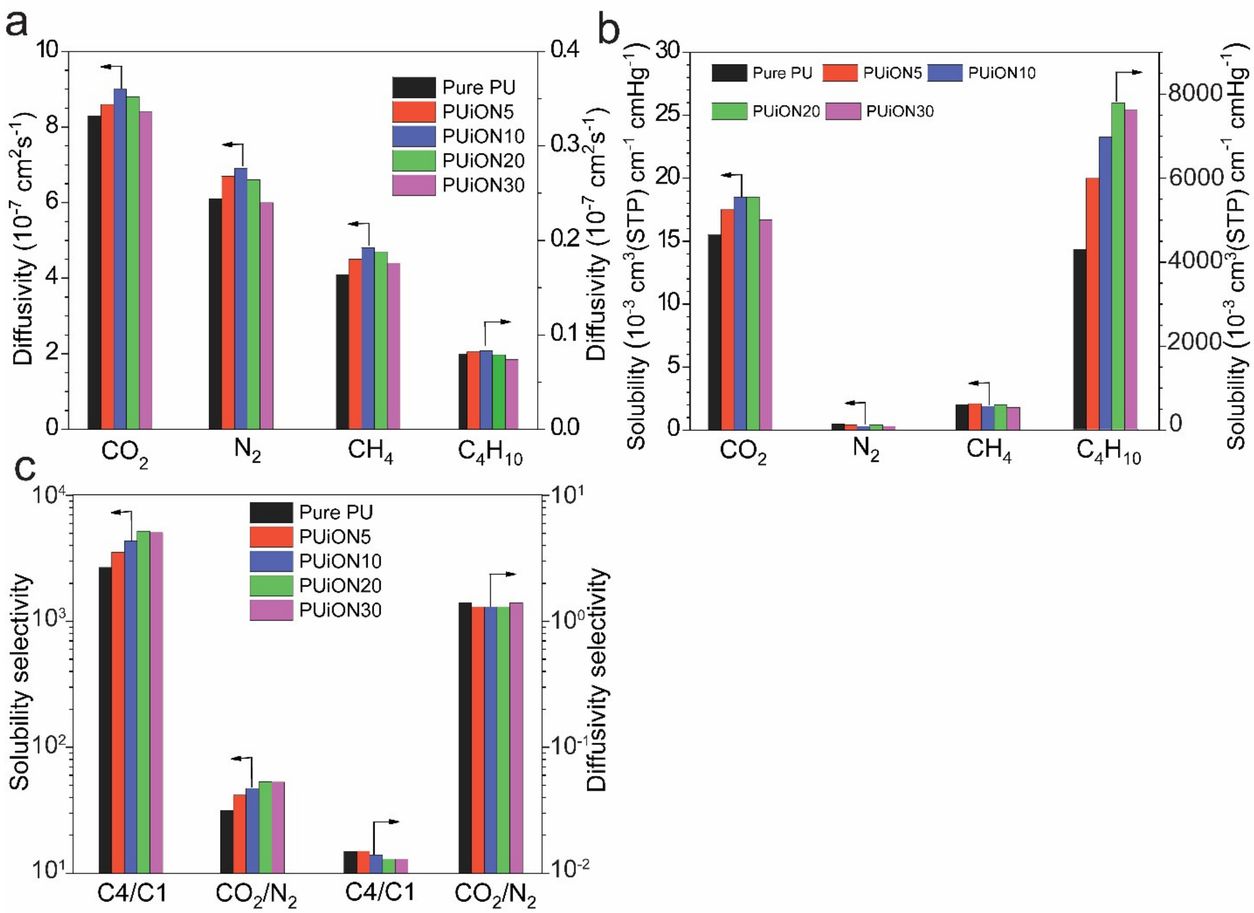

Fig. S5 (a) Diffusivity and (b) solubility coefficients of CO_2, N_2, CH_4 and C_4H_{10}, and (c) diffusivity and solubility selectivity of CO_2/N_2, C_4H_{10}/CH_4 in PU MMMs at different UiO66-NH2 loadings.

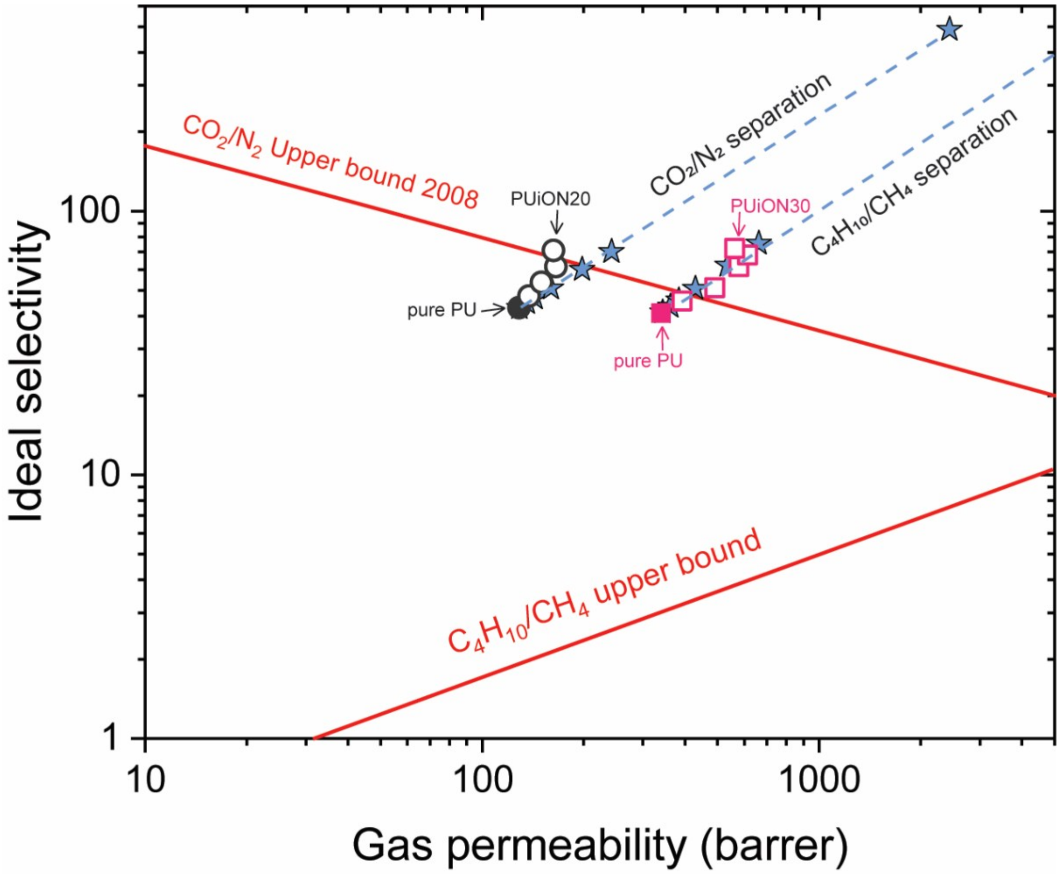

Fig. S6 Maxwell model prediction (dashed line) for CO_2/N_2 and C_4H_{10}/CH_4 separation. Pure permeability of UiO66-NH2 for each gas is predicted using the experimental data at low loadings (P_{N2}=30 barrer, P_{CH4}=37 barrer, P_{CO2}=2442 barrer , P_{C4H10}=8903 barrer). Pure gas permeability of the neat PU membrane and UiO66-NH2 particles are then used to predict the gas permeability of MMMs at diffetent loadings (blue stars). C_4H_{10}/CH_4 separation properties of PUiON membranes at different loadings (open dark pink square) are well predicted by the model at low filler concentrations. CO_2/N_2 separation properties of PUiON membranes at different loadings (open black circle) are almost matched with the Maxwell model data points (bule stars).

Supplementary information

Table S1: The HBI values of the membranes calculated from FTIR spectra

Samples	**PU**	**PU-UiON2.5**	**PU-UiON5**	**PU-UiON10**	**PU-UiON20**	**PU-UiON30**
HBI values	1.1	2.0	2.3	2.3	2.7	2.9

Table 2: Gas permeability and ideal selectivity in the PU/UiO66-NH2 MMMs at 4bar and 25°C. The butane permeability was measured at 1bar. The mixed gas data for C4H10/CH4 (50/50 vol.%) gas mixture are reported in parentheses.

Samples	Permeability (barrer)					Selectivity		
	CH_4	C_2H_6	C_3H_8	C_3H_6	C_4H_{10}	C_4H_{10}/CH_4	C_3H_8/CH_4	C_2H_6/CH_4
PU	8.3±0.7 (4.6)	21.6±1.3	63.8±3.2	161.4±8.5	343.6±24.0 (131.9)	41.4±4.5 (28.5)	7.7±0.8	2.6±0.3
PU-UiON2.5	8.6±0.7	23.1±1.2	69.0±2.9	180.2±9.4	392.5±25.5	45.6±4.8	8.0±0.7	2.7±0.3
PU-UiON5	9.6±0.8 (5.1)	27.5±1.4	87.5±5.2	215.6±13.1	490.3±34.8 (193.1)	51.1±5.6 (38.0)	9.1±0.9	2.9±0.3
PU-UiON10	9.4±0.8	30.0±2.1	91.2±6.4	238.6±15.3	578.0±35.8	61.5±6.5	9.7±1.1	3.2±0.4
PU-UiON20	9.0±0.7 (5.2)	30.5±1.9	90.2±5.6	245.0±14.0	613.6±36.2 (266.0)	68.2±6.7 (51.1)	10.0±1.1	3.4±0.4
PU-UiON30	7.8±0.5	26.5±1.4	84.7±5.5	231.9±15.1	563.0±29.8	72.2±6.0	10.9±1.0	3.4±0.3

Table 3: Gas permeability and ideal selectivity of the PU/UiO66-NH2 MMMs at 4bar and 25°C. The mixed gas data for CO_2/N_2 (50/50 vol.%) and CO_2/H_2 (50/50 vol.%) gas mixtures are reported in parentheses.

Samples	Permeability (barrer)					Selectivity		
	CO_2	H_2	O_2	N_2	CH_4	CO_2/H_2	CO_2/N_2	CO_2/CH_4
PU	129.1±9.0 (73.8)	15.8±1.1 (11.3)	10.1±0.8	3.0±0.2 (2.4)	8.3±0.7	8.2±0.8 (6.5)	43.0±4.3 (30.7)	15.6±1.7
PU-UiON2.5	138.0±10.3	15.8±1.2	9.8±0.8	2.9±0.2	8.6±0.7	8.7±0.9	47.6±5.0	16.0±1.8
PU-UiON5	150.2±11.7 (105.5)	15.7±1.2 (12.0)	9.4±0.6	2.8±0.2 (2.3)	9.6±0.8	9.6±1.0 (8.8)	53.6±5.9 (45.3)	15.6±1.8
PU-UiON10	166.4±13.3	15.2±1.1	8.8±0.7	2.7±0.2	9.4±0.8	10.9±1.2	61.6±7.0	17.7±2.1
PU-UiON20	163.0±13.2 (124.1)	14.8±1.2 (12.8)	7.6±0.5	2.3±0.2 (2.0)	9.0±0.7	11.0±1.3 (9.7)	70.9±8.1 (62.6)	18.1±2.0
PU-UiON30	140.6±9.5	13.2±1.0	6.5±0.3	1.9±0.1	7.8±0.5	10.7±1.0	72.3±7.1	18.0±1.7

Table S4: Molecular specification of penetrant gases [2]

Gas	Molecular size (Å)		Condensability (K)	
	d_{LJ}	D_k	T_b	ε/k
CO_2	4.00	3.30	195.0	190.0
O_2	3.43	3.46	90.2	113.0
N_2	3.68	3.64	77.4	91.5
CH_4	3.82	3.80	111.7	137.0
C_2H_6	4.42	-	184.5	230.0
C_3H_6	4.68	4.50	225.5	303.0
C_3H_8	5.06	4.30	231.1	254.0
C_4H_{10}	5.34	4.30	272.7	310.0

Table S5: N_2 permeability of the pure PU and PUiON10 and PUiON20 MMMs before and after C_4H_{10} permeation test at 1 bar

	N_2 permeability (barrer)			C_4H_{10}/N_2 selectivity		
samples	Pure PU	PUiON10	PUiON20	Pure PU	PUiON10	PUiON20
Before	3.0	2.7	2.3	114.5	214.1	266.8
After	3.8	2.8	2.2	90.4	209.4	281.2

1. A. P. Isfahani, B. Ghalei, K. Wakimoto, R. Bagheri, E. Sivaniah and M. Sadeghi, *J. Mater. Chem. A*, 2016, **4**, 17431-17439.
2. K. Tanaka, A. Taguchi, J. Hao, H. Kita and K. Okamoto, *J. Membr. Sci.*, 1996, **121**, 197-207.